Earth and Planetary Science Letters 284 (2009) 417–425

Contents lists available at ScienceDirect

Earth and Planetary Science Letters

journal homepage: www.elsevier.com/locate/epsl

Cosmogenic ^{3}He and ^{21}Ne measured in quartz targets after one year of exposure in the Swiss Alps

Pieter Vermeesch [a,*], Heinrich Baur [a], Veronika S. Heber [a,1], Florian Kober [a], Peter Oberholzer [a,2], Joerg M. Schaefer [a,3], Christian Schlüchter [b], Stefan Strasky [a,4], Rainer Wieler [a]

[a] Institute of Isotope Geology and Mineral Resources, ETH-Zurich, Switzerland
[b] Institute of Geological Sciences, University of Bern, Switzerland

ARTICLE INFO

Article history:
Received 19 March 2009
Received in revised form 4 May 2009
Accepted 5 May 2009
Available online 11 June 2009

Editor: R.W. Carlson

Keywords:
cosmogenic nuclides
attenuation length
neon
helium
quartz

ABSTRACT

All currently used scaling models for Terrestrial Cosmogenic Nuclide (TCN) production rates are based on neutron monitor surveys. Therefore, an assumption underlying all TCN studies is that production rates are directly proportional to secondary cosmic ray intensities for all cosmogenic nuclides. To test this crucial assumption, we measured cosmogenic ^{3}He and ^{21}Ne in artificial quartz targets after one year of exposure at mountain altitudes in the Swiss Alps. The targets were inconel steel tubes containing 1 kg of artificial quartz sand (250–500 μm), degassed for one week at 700 °C in vacuum prior to exposure. From August 2006 until August 2007, ten of these targets were exposed at five locations in Switzerland and Italy: Zürich (556 m), Davos (1560 m), Säntis (2502 m), Jungfraujoch (3571 m), and Monte Rosa (4554 m). Additionally, a sixth set of two blank targets was kept in storage and effectively shielded from cosmic ray exposure. Cosmogenic noble gases were measured at room temperature and at 700 °C. Up to 9% of the cosmogenic ^{3}He was measured in the cold step, indicating that ^{3}He diffuses out of quartz at room temperature on short time scales. The remaining ^{3}He and all ^{21}Ne were released at 700 °C, as shown by a repeat measurement at 800 °C for the Monte Rosa target, which yielded no additional cosmogenic helium and neon. As expected, the Monte Rosa target contained the highest cosmogenic nuclide content, with $1.56 \pm 0.07 \times 10^{6}$ atoms of excess ^{3}He and $4.5 \pm 1.2 \times 10^{5}$ atoms of excess ^{21}Ne (all errors are 2σ). The raw measurements were corrected for non-atmospheric blanks, shielding (roof + container wall), tritiogenic helium and solar modulation (normalised to the average neutron flux over the past five solar cycles). The ^{3}He/^{21}Ne production rate ratio of 6.8 ± 0.9 indicates that cosmogenic ^{3}He production by the container walls is negligible. The main goal of the artificial target experiment was to determine the production rate attenuation length. Because all our targets had an identical design and were exposed under identical conditions, all systematic errors cancel out in the calculation of an attenuation length. Our best estimates for the ^{3}He and ^{21}Ne attenuation lengths are 134.8 ± 5.9 g/cm^{2} and 135 ± 25 g/cm^{2}, respectively, agreeing very well with currently used scaling models. We conclude that TCN production rates are indeed proportional to neutron monitor count rates, and that ^{3}He and ^{21}Ne production rates follow the same altitudinal scaling relationships as the cosmogenic radionuclides. Finally, the measurements were scaled to sea level and high latitude using the empirical attenuation length, yielding weighted mean production rates of 107.6 ± 6.6 at/g/yr for ^{3}He and 15.4 ± 2.1 at/g/yr for ^{21}Ne. Despite the significant uncertainties associated with the corrections for shielding, solar modulation and especially the ^{3}He/^{3}H branching ratio, these estimates are in good agreement with production rates derived from long-term exposure experiments at natural calibration sites and physics-based simulations.

© 2009 Elsevier B.V. All rights reserved.

1. Introduction

All currently used scaling models for Terrestrial Cosmogenic Nuclide (TCN) production rates are based on neutron monitor surveys (Dunai, 2001; Lal, 1991; Stone, 2000; Dunai, 2000; Desilets and Zreda, 2003; Pigati and Lifton, 2004; Lifton et al., 2008). Therefore, an assumption underlying all cosmogenic nuclide studies is that production rates are directly proportional to secondary cosmic ray intensities for all cosmogenic nuclides. Several efforts are underway to test this crucial assumption by TCN production rate calibrations in the

* Corresponding author. Current affiliation: Birkbeck, University of London, United Kingdom. Tel.: +44 20 7679 3406.
E-mail address: p.vermeesch@ucl.ac.uk (P. Vermeesch).
[1] Current affiliation: Earth and Space Sciences, UCLA, Los Angeles, United States.
[2] Current affiliation: Baugeologie und Geo-Bau-Labor Chur, Switzerland.
[3] Current affiliation: Lamont Doherty Earth Observatory, United States.
[4] Current affiliation: Swiss Geological Survey, Switzerland.

0012-821X/$ – see front matter © 2009 Elsevier B.V. All rights reserved.
doi:10.1016/j.epsl.2009.05.007

framework of the CRONUS-EU and CRONUS-Earth initiatives. The bulk of this work is done on landforms of known age (Desilets and Zreda, 2006). These so-called 'natural calibration targets' are the method of choice for the calculation of accurate TCN production rates integrated over millennial time scales but are, unfortunately, often affected by poorly constrained factors such as shielding and erosion. It is notoriously hard to find vertical transects of natural calibration sites that allow the calculation of production rate attenuation lengths. Herein lies the complementary strength of artificial calibration targets. Because the exposure conditions of the latter are either known or constant, all systematic errors cancel out in the calculation of a production rate attenuation length. We here present the first results of an artificial target experiment measuring, for the first time, cosmogenic ^{3}He and ^{21}Ne in quartz after one year of exposure at mountain altitudes in the Swiss Alps. Previous artificial target experiments have mainly focused on water (Lal et al., 1960; Nishiizumi et al., 1996; Brown et al., 2000; Graham et al., 2000), although one pilot experiment used a silicate glass (Graf et al., 1996). We used quartz as the target material, because it is the most commonly used mineral for exposure dating and both cosmogenic helium and neon are produced and retained in the target container.

Our project has a history of more than ten years. A first target design was developed back in 1997. These were stainless steel containers with 14 cm radius and 45 cm height, filled with 4 kg of industrial quartz sand of natural origin (Fluka, no. 83340; Schäfer, 2000; Kober, 2004). The targets were heated to >800 °C under vacuum for a week in order to ensure complete degassing prior to exposure, and double sealed with a valve and copper tube clamp to prevent atmospheric leaks during exposure. Fourteen of these targets were exposed at seven different locations for two to four years. Two of them were measured, one unexposed blank target and one target that had been exposed at Jungfraujoch, at an altitude of 3571 m. The pilot experiment was aborted after the neon and helium compositions of these two targets were found to be a mixture of cosmogenic and other components (Kober, 2004). There are two reasons why the first target design failed. The presence of a 'trapped' component (neon plotting above the mixing line between atmospheric and cosmogenic components, the so-called 'spallation line'; Niedermann, 2002) indicates that pre-exposure degassing was insufficient, and that the quartz did not reach the 600 °C degassing temperature of neon (Niedermann, 2002). The presence of a 'nucleogenic' component (neon plotting below the spallation line) indicates that despite the purity of the industrial quartz sand, it still contained sufficient alpha producing U and Th (120 and 172 ppb, respectively) to compromise the helium and neon measurements. These observations led to the development of a second generation target design.

The effectiveness of the revised target design was verified in a custom-built prototype container (Section 1). Ten of these targets were exposed at different elevations in the Swiss Alps, at altitudes ranging from 556 to 4554 m (Section 2). Cosmogenic ^{3}He and ^{21}Ne were measured after one year of exposure, using a custom-built mass spectrometer and an optimised measurement routine (Section 3). Data reduction included corrections for non-atmospheric blanks, shielding, solar modulation, and tritiogenic helium (Section 3). ^{3}He and ^{21}Ne were measured in two steps at room temperature and at 700 °C. Most of the ^{3}He and all of the ^{21}Ne were measured in the hot step (Section 4). The altitude dependency of the TCN production rates was quantified by plotting them against atmospheric depth, yielding attenuation lengths that are in perfect agreement with existing scaling models (Section 5). Production rates were scaled to sea level and high latitude and agree well with previous determinations on natural calibration sites (Section 6). We conclude this paper with an outlook to the future, when duplicate artificial targets will be used to determine the ^{3}He/^{3}H branching ratio and we will monitor cosmogenic noble gas production rates over an entire solar cycle (Section 7).

2. Methods

2.1. Target design

The first generation targets suffered from sub-optimal degassing and impure quartz (Section 1). Both of these problems were addressed in the second generation target design. To eliminate the trapped neon component and ensure optimal degassing, the radius of the seamless stainless steel (grade 1.4301) canisters was reduced from 14 to 6 cm (Fig. 1.c), and in order to eliminate the nucleogenic component, we used artificially grown quartz crystals of optimal purity (supplied by Morion Company, USA), which were crushed to 250–500 μm sand size (Fig. 1.a), and rinsed with water and acetone. Gamma ray spectrometry measurements revealed U and Th concentrations <16 and <49 ppb, respectively, which is below the detection limit of the method and also below the levels measured in the Fluka quartz sand (Strasky, 2008). To verify the effectiveness of the new target design, two thermocouples were installed in a prototype container filled with 800 g quartz sand (Fig. 1.c). After a heating period of ~2.5 h at an external temperature of 900 °C, the temperature reached by the quartz in the innermost part of the container was ~850 °C, well above the degassing temperatures of helium and neon (Niedermann, 2002) (Fig. 1.d). To reduce the blank, the external temperature for the actual target measurements was later reduced to 700 °C, which should yield ~650 °C quartz temperatures. As was the case for the first generation (Section 1), also the second generation targets were double sealed by a 'bellows-sealed' Swagelok® valve connected to a copper tube with a stainless steel pinch-off clamp.

2.2. Pre-treatment and installation

One kg of the artificial quartz sand was degassed inside the targets for one week at 700 °C in vacuum prior to exposure using a custom-built furnace (Fig. 1.b). The targets were rolled in bubble wrap and placed in fibreglass cable trays for protection against the weather, and were installed in a horizontal position to minimise self-shielding. In August of 2006, two targets were exposed at each of five locations: Zürich (556 m), Davos (1560 m), Säntis (2502 m), Jungfraujoch (3571 m), and Monte Rosa (4554 m). All of these locations (except for Monte Rosa) are meteorological observatories of the Swiss Federal Office of Meteorology and Climatology (MeteoSwiss), which were kept snow-free during the winter of 2006–2007. The Zürich, Davos, and Säntis targets were installed outside and secured to the railings of the meteorological equipment. Because of the extremely high wind speeds at the Jungfraujoch and Monte Rosa sites, those targets were kept inside. Additionally, a sixth set of two blank targets was stored in the basement of a 10-storey building housing the ETH noble gas laboratory, ~15 m below street level, and effectively shielded from cosmic ray exposure. Exactly one year later, the targets were retrieved and subsequently measured.

2.3. Measurements

Even in 1 kg of quartz and at mountain altitudes, the expected amounts of cosmogenic gas are extremely low, on the order of tens of thousands of atoms in a volume of more than 4 l. To measure such minute amounts of noble gases, we used a unique kind of mass spectrometer developed at ETH-Zürich, which is equipped with a compressor source (Baur, 1999). The compressor consists of a magnetically levitated rotor, spinning at 1500 Hz, which forces the gas along spiral grooves in the inner wall of the stator. The neutral gas then enters the ionization volume and gets accelerated towards the magnet and ion detectors. The compressor source acts as a pump, consuming a much larger portion of the sample gas than a conventional mass spectrometer, and resulting in a two orders of magnitude gain in sensitivity.

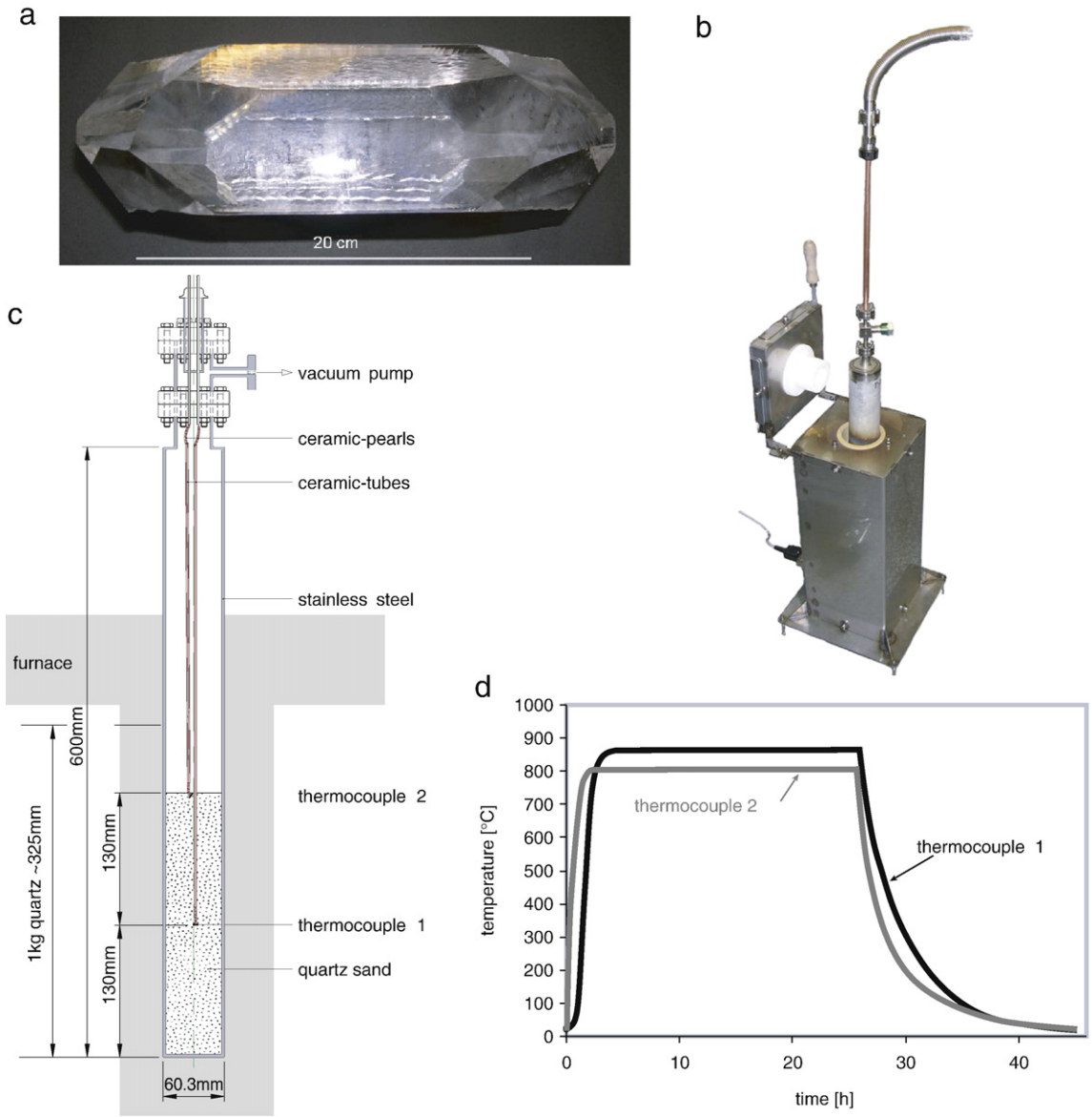

Fig. 1. a — Target material: artificially grown single quartz crystal before crushing. b — Custom-built furnace for quartz degassing. Note that the pinch-off clamp (missing in the picture) is mounted and closed before decoupling the target from the system. c — Prototype container outfitted with two thermocouples to verify thermal equilibration. d — After 2 h of heating at an external temperature of 900 °C, the internal parts of the quartz in the prototype container reach a temperature of ~850 °C, ensuring complete degassing of both neon and helium.

Cosmogenic noble gases were measured in two steps at room temperature and 700 °C. Before commencing the measurements, the connection of the artificial targets to the gas preparation line via the copper tube and a flexible bellow was baked and degassed for 24 h. Pressure in the extraction line and mass spectrometer was maintained at ultrahigh vacuum conditions of $\sim 10^{-10}$ mbar. To protect the extraction line and mass spectrometer against potential atmospheric leaks, a 'dummy run' was made by measuring the gas between the stainless steel pinch-off and the valve. Because the amount of this gas was always very small (~20,000 atoms ^{3}He) and had an atmospheric composition (^{3}He/^{4}He$\approx 2.1 \pm 0.9 \times 10^{-6}$), it is not reported in the data tables. Next, the valve was opened and the target volume equilibrated with a cold finger filled with activated charcoal and cooled by liquid N_2 for 15 min before releasing the gas into the gas purification line, where it was cleaned by one Ag and three Zr/Ti getters and two additional cold fingers for 30 min. Neon and helium were measured separately by freezing the neon to a cryogenic trap at 12.7 K for 15 min. The gas was expanded into the mass spectrometer while exposed to a final cold finger and getter. To monitor the sensitivity of the mass spectrometer (which changed <2%/day), calibrations ('fast cals') were done every morning and evening, using a fixed gas amount of an internal lab standard.

The sample gas was pumped into the ionization volume by the aforementioned magnetically levitated compressor, ionized by a Baur–Signer source (Baur, 1980) and accelerated through a magnetic sector mass spectrometer with a trajectory radius of 210 mm and mass resolution set to 600 in order to resolve ^{3}He from the HD molecule. The ^{3}He signal was digitally measured on an ion counter in 20 steps of 60 s while ^{4}He was measured in analogue mode on a Faraday cup in 20 steps of 40 s. These long measurement times were necessary to overcome the relatively poor counting statistics associated with our extremely low signals. Extrapolation to the time of gas inlet was achieved by linear regression of the data. Next, the remaining helium was pumped away and the cryogenic trap heated to 50 K in order to release the neon. Whereas the helium isotopes were simultaneously analysed, ^{20}Ne,

Table 1
Helium measurements (atoms) in chronological order of measurement.

Location	T (°C)	^{3}He ($\times 10^3$)	2σ	^{4}He ($\times 10^7$)	2σ	3/4 ($\times 10^{-6}$)	2σ	^{3}He† ($\times 10^3$)	2σ	^{3}He‡ ($\times 10^3$)	2σ
Blank (T13)	20	66.3	6.6	374	11	17.7	1.9	61.1	6.6	0	10
	700	14.6	4.9	442	13	3.3	1.1	8.4	4.9	0	7.0
Jungfrau (T10)	20	149	13	478	14	31.3	2.8	143	13	65	16
	700	745	41	430	13	173	11	740	40	731	41
Monte Rosa (T12)	20	160	11	377	11	42.5	3.2	155	11	93	13
	700	1488	70	593	17	251	14	1479	70	1468	71
	800	9.1	4.0	438	13	2.1	0.9	2.9	4.0	2.9	4.0
Säntis (T8*)	20	174	17	806	23	21.6	2.2	163	17	31	23
	700	453	31	2804	81	16.1	1.2	413	31	360	44
Davos (T9)	20	81.2	8.4	424	12	19.2	2.1	75.3	8.4	6	12
	700	206	16	461	14	44.7	3.8	199	16	191	17
Säntis (T7)	20	83	12	444	17	18.7	2.9	77	12	4	15
	700	431	29	406	17	106.2	8.4	425	29	414	30
Zürich (T15**)	20	191	17	463	16	41.4	4.0	185	17	109	19
	700	195	21	586	20	33.2	3.8	187	21	170	23
Zürich (T2)	20	115.6	9.0	640	19	18.1	1.5	106.7	9.0	2	15
	700	123	16	430	13	28.6	3.8	117	16	104	17
Blank (T16***)	700	18.6	6.6	430	13	4.3	1.5	12.6	6.6	0	9.3

† — cosmogenic ^{3}He assuming an atmospheric blank; ‡ — cosmogenic ^{3}He using the measured blank; * — leaking target; ** — high residual blank in the mass spectrometer; *** — cold step lost.

^{22}Ne and ^{21}Ne were measured in peak jumping mode on the ion counter in 15 cycles of 20, 30 and 60 s, respectively. H_2O, ^{40}Ar and CO_2 were monitored and interference corrections were made for masses 20 (2‰ of H_2O and 0.45‰ of ^{40}Ar) and 22 (0.044‰ of CO_2). ^{20}Ne was extrapolated to the time of gas inlet by exponential regression. The ^{21}Ne and ^{22}Ne abundances were calculated by monitoring the ^{22}Ne/^{20}Ne and ^{21}Ne/^{20}Ne ratios over the course of each analysis. These so-called 'local ratios' were constant for the first five target measurements, which took place in November 2007. The remaining four targets were measured several months later as a result of technical problems unrelated to our experiment. The mass spectrometer behaved slightly differently when the measurements resumed, resulting in ^{22}Ne/^{20}Ne and ^{21}Ne/^{20}Ne local ratios that increased with time. To account for this change in behaviour, a new blank target (T16) was measured after completion of the final measurements, so as to ensure internal consistency of the target measurements and the blank-target based fractionation correction (Section 3.1).

After completion of the neon measurement, the cryogenic trap and mass spectrometer were isolated from the extraction line, the remaining 'cold' target gas was pumped away, and the furnace was switched on. An external temperature of 700 °C (corresponding to an internal temperature of ~650 °C, Fig. 1.d) was maintained for 5 h, after which the 'hot' measurement proceeded in exactly the same way as the 'cold' measurement described in the previous paragraph. In addition to the sensitivity calibrations, we also performed a set of abundance calibrations ('slow cals') by expanding a known volume of calibration gas into the extraction line, including the target volume. This was done at both room temperature and 700 °C, using exactly the same analytical procedure as for a real target measurement.

3. Data reduction

The raw measurements were in units of Amperes (^{4}He) and Hertz (all other nuclides). They were converted to atomic units by sensitivity and abundance calibrations (the aforementioned 'fast cals' and 'slow cals', respectively). The resulting values were corrected for non-atmospheric blanks, shielding, solar modulation and tritiogenic helium, following procedures described in the following paragraphs.

3.1. Blank corrections

Pressure inside the targets was $1–2\times10^{-2}$ mbar after one year of exposure. While this low pressure showcases the effectiveness of the pre-exposure degassing and the double seal, the inferred amounts of non-cosmogenic ^{3}He in the blank are far from trivial and must be corrected for. The easiest solution is to assume an atmospheric isotopic composition (column 9 of Table 1). However, the ^{3}He/^{4}He ratio for the cold step of blank target T13 was $17.7\pm1.9\times10^{-6}$, significantly higher than the atmospheric value ($1.399\pm0.013\times10^{-6}$, Porcelli et al., 2002). The hot steps were closer to atmosphere: $3.3\pm1.1\times10^{-6}$ for T13, and $4.3\pm1.5\times10^{-6}$ for a second blank target, T16 (column 7 of Table 1). The non-atmospheric helium compositions imply a fractionated blank, possibly due to diffusion of helium and/or tritium (Tilles, 1962) through the valves and container wall. We used the measured isotopic ratios of the blank targets for the blank correction of all our targets (column 11 of Table 1), and applied the same procedure for the neon measurements (column 15 of Table 2). The blank corrections have a strong effect on the low temperature helium measurements of the low-altitude targets (Zürich, Davos, Säntis); a moderate effect on the high-altitude targets

Table 2
Neon measurements, in atoms.

Location	T (°C)	^{20}Ne ($\times 10^6$)	2σ	^{21}Ne ($\times 10^3$)	2σ	^{22}Ne ($\times 10^6$)	2σ	21/20 ($\times 10^{-3}$)	2σ	22/20 ($\times 10^{-3}$)	2σ	^{21}Ne† ($\times 10^3$)	2σ	^{21}Ne‡ ($\times 10^3$)	2σ
T13	700	603	18	1768	55	61.2	1.8	2.93	0.13	101.5	4.3	−18	77	0	110
T10	700	266.3	7.9	998	33	26.85	0.80	3.75	0.17	100.8	4.2	210	40	218	52
T12	700	596	18	2184	68	61.4	1.8	3.66	0.16	103.0	4.3	420	86	440	110
	800	306.0	9.0	907	29	30.93	0.92	2.97	0.13	101.1	4.2	2	40	11	55
T9	700	176.9	5.2	585	19	18.16	0.53	3.31	0.14	102.6	4.3	61	24	66	33
T7	700	81.4	3.3	354	17	8.33	0.35	4.35	0.27	102.4	6.0	113	19	112	23
T15**	700	142.7	5.1	436	20	13.72	0.51	3.06	0.18	96.2	4.9	14	25	11	34
T2	700	53.3	3.5	182	13	5.58	0.36	3.41	0.32	104.6	9.6	24	16	23	18
T16***	700	46.3	1.4	137.8	6.1	4.66	0.16	2.98	0.16	100.6	4.6	0.8	7.4	0	11

Annotations as in Table 1.

(Jungfraujoch, Monte Rosa); and a minor effect on the high temperature measurements, including neon. Fortunately, most of the helium and all of the neon were released at high temperature (Section 4).

3.2. Shielding

No topographic shielding correction was required because all the high elevation targets were installed on the summits of mountains, and the low elevation targets (Zürich and Davos) were located in broad valleys. Snow cover was either removed or negligible. A 1.5% correction was associated with shielding by the container wall (2.6 mm steel) and an additional 1.5% with the roofs at the Monte Rosa and Jungfraujoch sites (2 mm aluminium plus 2 cm wood). A nominal uncertainty of 50% was assigned to these corrections.

3.3. Solar modulation

The experiment took place during a solar minimum, causing higher than normal production rates. One of our targets was installed adjacent to the IGY neutron monitor at the Jungfraujoch neutron observatory, which has been in continuous operation since 1958. We have scaled our results to the average neutron signal over the past four solar cycles. This correction lowered our longer term production rate estimates by 4.6% (Fig. 2).

3.4. Tritiogenic helium

The cosmogenic ^{3}He measured in natural samples is either directly derived from spallogenic reactions on heavier nuclides, or it is a secondary radiogenic product of spallogenic tritium. The half life of ^{3}H is 12.32 years, which is short compared to the time periods of interest in exposure dating, but long in comparison with the duration of our artificial target experiment. Therefore, the apparent ^{3}He production rates measured by our artificial targets are significantly lower than the effective ^{3}He production rate relevant to TCN studies. The relative amount of ^{3}He measured at a time t after the retrieval of a target that has been exposed for a time period T is given by:

$$\frac{\left[^3\mathrm{He}\right]_t}{\left[^3\mathrm{He}\right]_\infty} = 1 - \frac{e^{-\lambda t}\left(1 - e^{-\lambda T}\right)}{\lambda T(1 + B)}$$

where B is the ^{3}He/^{3}H branching ratio, which is unknown for spallation by neutrons, but has been estimated by simulation and proton-based accelerator experiments to be ~0.9 for Si and ~1.06 for O (Leya and Masarik, 2009). Therefore, we will assume $B = 1$ for quartz in the following.

In the case of water targets, it is straightforward to measure the branching ratio. Because tritium binds to oxygen in water, it is retained in the target during ^{3}He measurement. By remeasuring a target some time after release of the 'primary' ^{3}He, the amount of tritiogenic helium can be determined, and a branching ratio calculated (Brown et al., 2000). Things are somewhat more complicated for quartz targets, because some if not all of the tritium may escape during the heating step. Therefore, a second target is needed to estimate the ^{3}He/^{3}H branching ratio in quartz. Thus, our duplicate targets serve a dual purpose. In addition to allowing a backup solution for failed measurements, they also provide the only way to avoid making assumptions about the branching ratio. We intend to analyse those duplicate targets that have not yet been measured, especially the high-altitude targets from Monte Rosa and Jungfraujoch, five to ten years from now. In the meanwhile, it is still necessary to assume a branching ratio for the tritium-correction.

4. Results

Targets T13, T10, T12, T8 and T9 were measured in November 2007. Target T8 (Säntis) suffered from an atmospheric leak, causing anomalously high – but still measurable – pressures and raw signals significantly higher than those of the Monte Rosa target (Table 1). The leak precluded the ^{21}Ne measurement for T8, but after the blank correction, the ^{3}He signal was still meaningful albeit imprecise. In December 2007, following an accident unrelated to our experiment, the extraction line was contaminated with water, and the mass spectrometer was out of service for half a year. When the duplicate Säntis target (T7) was measured in July of 2008, sensitivity of the machine had dropped by a third. Sensitivity increased again by about 10% in September of 2008, but this was associated with a marked increase in the residual blank, which compromised the lowest elevation measurement (T15 — Zürich). After a thorough servicing of the extraction line and mass spectrometer, blanks were finally reduced and the sensitivity restored to the original levels. A duplicate Zürich measurement (T2) was made as well as an additional blank target (T16). The measurements of the 'failed' target measurements (T8 and T15) are given in Table 1 for the sake of completeness, but will not be considered in the remainder of this paper, which will use the duplicate target measurements (T7 and T2) instead. Therefore, in the following paragraphs, 'Säntis' is equivalent to 'target T7', and 'Zürich' is equivalent to 'target T2'.

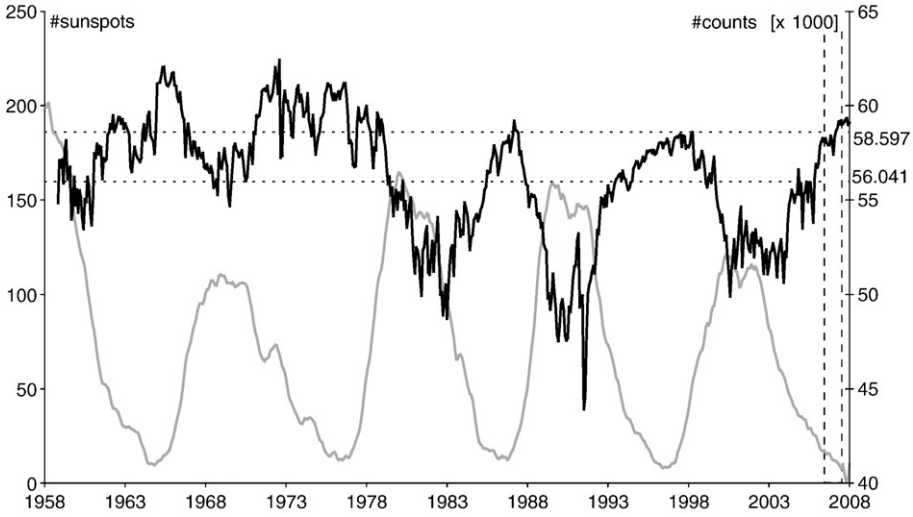

Fig. 2. Sunspot number (grey) and IGY neutron monitor counts at Jungfraujoch (black) over the past 50 years. The vertical dashed lines mark the exposure time of our targets, the horizontal dotted lines the average number of counts over the past five solar cycles (bottom) and the duration of the experiment (top).

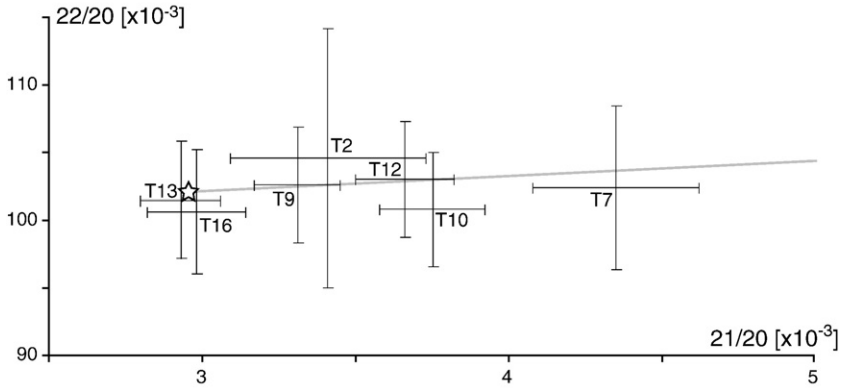

Fig. 3. Neon three-isotope plot (700 °C steps). The star marks the atmospheric composition, the spallation line is shown in grey (Niedermann, 2002). Error symbols are 2σ.

The helium release spectra indicate that between 1 and 9% of the cosmogenic ^{3}He was measured in the cold step (Table 1). This confirms earlier experiments indicating that ^{3}He quickly diffuses out of quartz at room temperature (Shuster and Farley, 2005). The remaining ^{3}He was released at 700 °C. The ^{3}He/^{4}He isotopic ratio systematically increases with elevation, which is a clear sign of cosmogenic helium production. Non-atmospheric blank corrections were 5% for the Monte Rosa target, 10% for Jungfraujoch, 30% for Säntis and Davos, and 50% for Zürich (Table 1). During the delay caused by the aforementioned technical problems, spallogenic ^{3}H in the targets decayed by about 5%, resulting in an equivalent change in the tritiogenic helium correction for the targets measured in 2008 (T7 and later), compared to the targets measured in 2007 (T9 and earlier).

Virtually no ^{21}Ne was measured in the cold step, with nearly all the cosmogenic ^{21}Ne being released at 700 °C. A re-extraction measurement at 800 °C for the Monte Rosa target showed that the small amount of gas that remained at that temperature had an atmospheric composition (Table 2). On the neon three-isotope plot, all targets are within 2σ from the spallation line (Fig. 3). The cold neon steps (not shown) and blank targets (T13 and T16) have an atmospheric composition. Precision of the Zürich target (T2) was insufficient to distinguish it from the atmosphere, reflecting the limits of our target design. Both in the blanks and in the 800 °C re-extraction, the neon composition is slightly fractionated. This is consistent with the (much stronger) fractionation observed for helium. Blank corrections for neon were less than 5% except for the Davos target (8%). This is much smaller than the helium blank corrections. Furthermore, blank corrections are inherently 'safer' for neon than helium because the former has three isotopes, facilitating the detection of non-atmospheric components (Fig. 3). So whereas neon is more challenging to measure than helium due to the lower production rates and higher degassing temperature, the data reduction is easier because blanks are less of an issue, and there is no significant radiogenic source.

Although an empty target container (exposed in Tibet since 2005) was not retrieved for logistical reasons, it is possible to evaluate the production of cosmogenic noble gases from the container walls by considering the ^{3}He/^{21}Ne production rate ratio. We may safely assume that ^{3}He would be affected more than ^{21}Ne, first because steel/quartz production rate ratios are considerably higher for ^{3}He than for ^{21}Ne and second because helium should diffuse more efficiently from the walls into the container than neon. Hence, the ^{3}He/^{21}Ne ratio in the empty targets should be higher than the quartz value. The weighted mean of our measured ^{3}He/^{21}Ne ratios is 6.8 ± 0.9 (2σ) whereas in natural quartz it may be about 6.7 (Masarik and Reedy, 1995). Thus, we believe that although some of the measured ^{3}He and ^{21}Ne may come from the container, this fraction is small. At any rate, it is unimportant for the calculation of a production rate attenuation length, which is discussed next.

5. Attenuation lengths

The main goal of the artificial target experiment was to determine the production rate attenuation length. Because all our targets had an identical design and were exposed under identical conditions, all systematic errors should cancel out in the calculation of an attenuation length. After scaling the measurements to a common reference latitude (Davos) using the latitudinal scaling model of Desilets et al. (2006), our best estimates are 134.6 ± 5.9 g/cm^2 for the ^{3}He attenuation length and 135 ± 25 g/cm^2 for the ^{21}Ne attenuation length (Fig. 4). The MSWDs of 1.9 and 0.32 indicate slight over- and underdispersion for ^{3}He and ^{21}Ne,

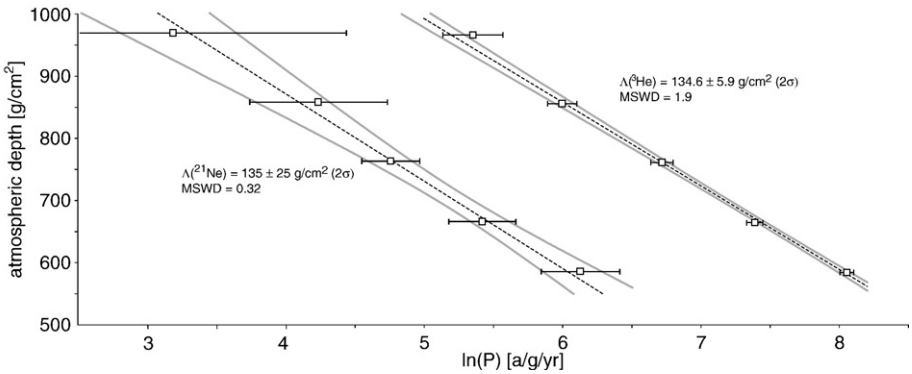

Fig. 4. Production rate attenuation lengths for ^{3}He (right) and ^{21}Ne (left). Error bars are 2σ. Targets are, from top to bottom: Zürich (T2), Davos (T9), Säntis (T7), Jungfraujoch (T10), and Monte Rosa (T12).

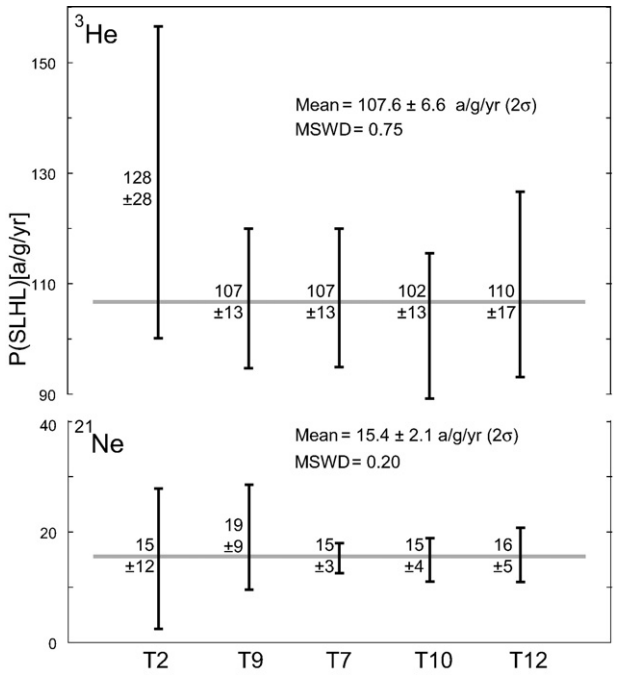

Fig. 5. Solar modulation corrected production rates at sea level and high latitude for ^{3}He (top) and ^{21}Ne (bottom). Error bars are 2σ, the grey lines represent the weighted means.

respectively (McIntyre et al., 1966). Overall, the fit is very good and the precision of the attenuation lengths (4% for ^{3}He) is comparable to or better than that obtained by natural calibration experiments (Desilets and Zreda, 2006). In order to compare our attenuation length estimates with existing scaling models, the reference cutoff rigidity of 4.36 GV was converted to an equivalent dipolar geomagnetic latitude of 43.47° and geomagnetic inclination of 62.19°. Using these latitudinal parameters, scaling factors were calculated for the atmospheric depths of our target locations according to various scaling procedures, and for each scaling procedure a single exponential curve was fitted to the synthetic data, exactly as was done for the actual target measurements. The resulting attenuation lengths compare favourably with our estimates, ranging from 146 g/cm^2 (Lal, 1991; Stone, 2000) to 131 g/cm^2 (Dunai, 2000; Desilets and Zreda, 2003) and 133 g/cm^2 (Desilets et al., 2006). All calculations were done using CosmoCalc 1.4 (Vermeesch, 2007).

6. Production rates

Determining cosmogenic noble gas production rates from artificial quartz targets is challenging because of the substantial uncertainties associated with the various corrections (Section 3). This is especially the case for the ^{3}He/^{3}H branching ratio which, as explained before, we have assumed to be one (Section 4). Given these caveats, the production rate estimates are remarkably consistent with previous determinations.

The corrected measurements were scaled to sea level and high latitude (SLHL) using the empirical ^{3}He attenuation length of 134.6 ± 5.9 g/cm^2 and cutoff rigidity values provided by the University of Bern (http://cosray.unibe.ch). The five ^{3}He production rate estimates scatter between 102 and 128 at/g/yr, with analytical uncertainties between 11% (Säntis) and 21% (Zürich) (Fig. 5; Table 3). The weighted mean production rate of 107.6 ± 6.6 at/g/yr is in good agreement with physics-based model calculations (Masarik and Reedy, 1995). The observed scatter is well explained by the analytical uncertainty alone, as indicated by the MSWD of 0.75.

The ^{21}Ne production rate estimates range from 15 to 19 at/g/yr, with analytical uncertainties of 22 to 80%, which is substantially larger than the helium production rate uncertainties. The relatively low MSWD (0.20) indicates underdispersion and, therefore, the neon uncertainties are probably somewhat overestimated. The weighted mean of the five production rate estimates is 15.4 ± 2.1 at/g/yr, which is also close to the accepted values (Niedermann et al., 1994; Masarik and Reedy, 1995; Niedermann, 2000; Amidon et al., 2009; Goethals et al., 2009),

Table 3
Data reduction for ^{3}He and ^{21}Ne.

Location	Monte Rosa (T12)	Jungfrau (T10)	Säntis (T7)	Davos (T9)	Zürich (T2)
Latitude	45.94	46.55	47.25	46.80	47.37
Longitude	7.87	7.98	9.34	9.84	8.54
Elevation	4554	3571	2502	1560	560
Date closed	02/08/2006	26/07/2006	25/04/2006	10/06/2006	02/08/2006
Exposed	25/08/2006	24/08/2006	05/09/2006	05/09/2006	06/09/2006
Retrieved	01/09/2007	27/08/2007	29/08/2007	29/08/2007	24/08/2007
Measured	26/11/2007	24/11/2007	07/07/2008	30/11/2007	05/11/2008
# years	1.018	1.008	0.980	0.980	0.964
Shielding	0.963	0.963	0.985	0.985	0.985
^{3}He [$\times 10^{3}$]	1561	796	418	197	107
2σ	72	44	34	21	23
$^{3}He_t/^{3}He_\infty$	0.520	0.521	0.536	0.520	0.545
$P(^{3}He)$	3064	1576	807	392	206
2σ	155	93	65	42	45
^{21}Ne [$\times 10^{3}$]	450	225	116	69	24
2σ	120	54	24	34	19
$P(^{21}Ne)$	450	225	116	69	24
2σ	120	54	24	34	19
R_c	4.69	4.46	4.19	4.36	4.15
Atm depth	584	664	761	856	966
S_λ	0.90	0.91	0.92	0.92	0.93
S_z	29.5	16.2	7.78	3.80	1.659
2σ	4.3	1.9	0.68	0.22	0.036
$P(^{3}He)_{SLHL}$	110	102	107	107	128
2σ	17	13	13	13	28
$P(^{21}Ne)_{SLHL}$	16.0	14.6	15.4	18.9	15
2σ	4.8	3.9	3.5	9.4	12

$P(\cdot)$ = production rates in at/g/yr, R_c = cutoff rigidity in GV, S_λ = latitudinal scaling factor, S_z = altitudinal scaling factor. Elevation in metres, atmospheric depth in g/cm^2, ^{3}He and ^{21}Ne in atoms. The SLHL production rates (bottom) were corrected for solar modulation, the raw production rates (middle) were not.

especially considering that solar activity has been considerably higher over the past five decades than during the 11,000 years before that (Solanki et al., 2004), causing lower than normal instantaneous TCN production rates.

7. Conclusions and outlook

We successfully measured cosmogenic ^{3}He and ^{21}Ne in quartz after one year of exposure in the Swiss Alps. After correcting for non-atmospheric blanks, shielding, tritiogenic helium production and solar modulation, the cosmogenic noble gas production rates agree well with previous determinations. Production rates, however, were not our primary concern for two reasons. First, it is hard to rule out all systematic errors associated with the aforementioned corrections. Second, production rates vary greatly over time in response to changes in the Earth's magnetic field and variations in solar activity, making it difficult to compare short- and long-term production rates with each other. Nevertheless, the good agreement of our production rate estimates with previous determinations, and particularly the ^{3}He/^{21}Ne production rate ratio, gives us great confidence in the robustness of our method. The main strength of artificial target experiments is in measuring attenuation lengths, again for two reasons. First, all systematic errors cancel out in the calculation of an attenuation length. Second, our short-term attenuation length estimates can be directly compared with short-term neutron monitor surveys. The excellent agreement between the former and the latter indicates that neutron monitors are indeed a good basis for production rate scaling models. And in contrast to what others have suggested (Amidon et al., 2008), altitudinal scaling of noble gases also appears to be identical to that of other cosmogenic nuclides, such as ^{36}Cl or ^{10}Be. These simplifying results are a nice departure from many other recent developments in cosmogenic nuclide science, which has rapidly grown increasingly complex over the past few years (Lifton, 2004; Pigati and Staiger et al., 2007; Lifton et al., 2008).

This is an ongoing experiment. As discussed before, the duplicate targets of Monte Rosa, Jungfraujoch, and Davos have not yet been measured and are kept shielded from cosmic rays. Measuring the ^{3}He content of these targets in a few years time will provide a direct estimate of the ^{3}He/^{3}H branching ratio in quartz. As an added bonus, because the temperature in the storage room is constant, the amount of ^{3}He measured in the cold step relative to that measured in the hot step will put further constraints on the ease of diffusion of cosmogenic helium out of quartz at room temperature (Shuster and Farley, 2005). During the summer of 2007, the targets reported in this paper were replaced by a new set of identical targets. These replacement targets have two purposes. First, they will be exposed for longer than one year, which will further improve the precision of our experiment. Second, subsequent replacements will track an entire solar cycle by sequential artificial target measurements over the next decade.

The precision of our attenuation length measurements rivals that of natural calibration samples, and the accuracy is likely to be better, as our artificial targets circumvent the geological problems (erosion, snow, and vegetation cover) affecting natural targets. Furthermore, our artificial targets can be used anywhere on the planet, whereas suitable lithologies and exposure histories for natural calibration experiments are rare. Nevertheless, natural calibration sites are still useful as they integrate cosmogenic nuclide production over millennial time scales that are more relevant to exposure dating than the one year time scale of our experiment. Thus, natural and artificial targets have complementary strengths which, together, can be used to further test and improve scaling models.

Acknowledgments

Swift yet detailed reviews by William Amidon (Caltech) and Samuel Niedermann (GFZ Potsdam) are gratefully acknowledged. PV would also like to thank Rolf Bütikofer (University of Bern) for providing the neutron monitor measurements (Fig. 2), Louise Wilson (University of Bern) for the permits to access the Jungfraujoch neutron observatory, Arthur Kunz (MeteoSwiss) for granting access to meteorological stations at all target locations below Monte Rosa, and Giorgio Tiraboschi (Club Alpino Italiano) for granting access to the Cabana Margarita on Monte Rosa. This work was financially supported by Swiss Nationalfonds Grant No. 200020-105220/1 and a Marie Curie Fellowship of the European Union (CRONUS-EU network, RTN project reference 511927).

References

Amidon, W., Farley, K., Burbank, D., Pratt-Sitaula, B., 2008. Anomalous cosmogenic ^{3}He production and elevation scaling in the high Himalaya. Earth Planet. Sci. Lett. 265 (1–2), 287–301.

Amidon, W., Rood, D., Farley, K., (2009). Cosmogenic ^{3}He and ^{21}Ne production rates calibrated against ^{10}Be in minerals from the Coso volcanic field. Earth Planet. Sci. Lett. 280, 194–204.

Baur, H., 1980. Numerische simulation und praktische erprobung einer rotationssymmetrischen ionenquelle für gasmassenspektrometer. Ph.D. Thesis, ETH-Zürich No. 6596.

Baur, H., 1999. A noble-gas mass spectrometer compressor source with two orders of magnitude improvement in sensitivity. EOS, Trans. — Am. Geophys. Union 80, F1118.

Brown, E.T., Trull, T.W., Jean-Baptiste, P., Raisbeck, G., Bourlès, D., Yiou, F., Marty, B., 2000. Determination of cosmogenic production rates of ^{10}Be, ^{3}He and ^{3}H in water. Nucl. Instrum. Methods Phys. Res., B Beam Interact. Mater. Atoms 172, 873–883.

Desilets, D., Zreda, M., 2003. Spatial and temporal distribution of secondary cosmic-ray nucleon intensities and applications to in situ cosmogenic dating. Earth Planet. Sci. Lett. 206, 21–42.

Desilets, D., Zreda, M., 2006. Elevation dependence of cosmogenic ^{36}Cl production in Hawaiian lava flows. Earth Planet. Sci. Lett. 246, 277–287.

Desilets, D., Zreda, M., Prabu, T., 2006. Extended scaling factors for in situ cosmogenic nuclides: new measurements at low latitude. Earth Planet. Sci. Lett. 246, 265–276.

Dunai, T., 2000. Scaling factors for production rates of in situ produced cosmogenic nuclides: a critical reevaluation. Earth Planet. Sci. Lett. 176, 157–169.

Dunai, T., 2001. Influence of secular variation of the geomagnetic field on production rates of in situ produced cosmogenic nuclides. Earth Planet. Sci. Lett. 193, 197–212.

Goethals, M.M., Hetzel, R., Niedermann, S., Wittmann, H., Fenton, C.R., Christl, M., Kubik, P.W., von Blanckenburg, F., 2009. An accurate experimental determination of cosmogenic ^{10}Be/^{21}Ne and ^{26}Al/^{21}Ne production ratios in quartz. Earth Planet. Sci. Lett. doi:1016/j.epsl.2009.04.027.

Graf, T., Marti, K., Wiens, R., 1996. The ^{21}Ne production rate in a Si target at mountain altitudes. Radiocarbon 38, 155.

Graham, I.J., Barry, B.J., Ditchburn, R.G., Whitehead, N.E., 2000. Validation of cosmogenic nuclide production rate scaling factors through direct measurement. Nucl. Instrum. Methods Phys. Res., B Beam Interact. Mater. Atoms 172, 802–805.

Kober, F., 2004. Quantitative analysis of the topographic evolution of the Andes of northern Chile using cosmogenic nuclides. PhD thesis, ETH-Zürich No. 15858.

Lal, D., 1991. Cosmic ray labelling of erosion surfaces: *in situ* nuclide production rates and erosion models. Earth Planet. Sci. Lett. 104, 424–439.

Lal, D., Arnold, J., Honda, M., 1960. Cosmic-ray production rates of Be^{7} in oxygen, and P^{32}, P^{33}, S^{35} in argon at mountain altitudes. Phys. Rev. 118 (6), 1626–1632.

Leya, I., Masarik, J., 2009. Cosmogenic nuclides in stony meteorites revisited. Meteorit. Planet. Sci. (in revision).

Lifton, N., Smart, D.F., Shea, M.A., 2008. Scaling time-integrated in situ cosmogenic nuclide production rates using a continuous magnetic model. Earth Planet. Sci. Lett. 268, 190–201.

Masarik, J., Reedy, R.C., 1995. Terrestrial cosmogenic-nuclide production systematics calculated from numerical simulations. Earth Planet. Sci. Lett. 136, 381–395.

McIntyre, G.A., Brooks, C., Compston, W., Turek, A., 1966. The statistical assessment of Rb–Sr isochrons. J. Geophys. Res. 71, 5459–5468.

Niedermann, S., 2000. The ^{21}Ne production rate in quartz revisited. Earth Planet. Sci. Lett. 183, 361–364.

Niedermann, S., 2002. Cosmic-ray-produced noble gases in terrestrial rocks: dating tools for surface processes. Rev. Mineral. Geochem. 47.

Niedermann, S., Graf, T., Kim, J., Kohl, C., Marti, K., Nishiizumi, K., 1994. Cosmic-ray-produced ^{21}Ne in terrestrial quartz: the neon inventory of Sierra Nevada quartz separates. Earth Planet. Sci. Lett. 125 (1–4), 341–355.

Nishiizumi, K., Finkel, R.C., Klein, J., Kohl, C., 1996. Cosmogenic production of ^{7}Be and ^{10}Be in water targets. J. Geophys. Res. 101, 22,225–22,232.

Pigati, J., Lifton, N., 2004. Geomagnetic effects on time-integrated cosmogenic nuclide production with emphasis on in situ ^{14}C and ^{10}Be. Earth Planet. Sci. Lett. 226, 193–205.

Porcelli, D., Ballentine, C.J., Wieler, R., 2002. An overview of noble gas geochemistry and cosmochemistry. Rev. Mineral. Geochem. 47.

Schäfer, J.M., 2000. Reconstruction of landscape evolution and continental paleoglaciations using in situ cosmogenic nuclides. Ph.D. Thesis, ETH-Zürich No. 13542.

Shuster, D., Farley, K., 2005. Diffusion kinetics of proton-induced ^{21}Ne, ^{3}He, and ^{4}He in quartz. Geochim. Cosmochim. Acta 69, 2349–2359.

Solanki, S.K., Usoskin, I.G., Kromer, B., Schüssler, M., Beer, J., 2004. Unusual activity of the Sun during recent decades compared to the previous 11,000 years. Nature 431, 1084–1087.
Staiger, J., Gosse, J., Toracinta, R., Oglesby, B., Fastook, J., Johnson, J.V., 2007. Atmospheric scaling of cosmogenic nuclide production: climate effect. J. Geophys. Res. (Solid Earth) 112, B2205.
Stone, J.O., 2000. Air pressure and cosmogenic isotope production. J. Geophys. Res. 105, 23,753–23,759.
Strasky, S., 2008. Glacial response to global climate changes: cosmogenic nuclide chronologies from high and low latitudes. Ph.D. Thesis, ETH-Zürich No. 17569.
Tilles, D., 1962. A room-temperature diffusion constant for hydrogen in proton-irradiated steel. Nature 194 (4835), 1273–1274.
Vermeesch, P., 2007. CosmoCalc: an Excel add-in for cosmogenic nuclide calculations. Geochem. Geophys. Geosyst. 8, 8003.